Composites Science and Technology 87 (2013) 204–209

Contents lists available at ScienceDirect

Composites Science and Technology

journal homepage: www.elsevier.com/locate/compscitech

High temperature thermomechanical behavior of silica-phenolic composite exposed to heat flux environments

Shengbo Shi, Jun Liang *, Guochang Lin, Guodong Fang

Science and Technology on Advanced Composites in Special Environments Key Laboratory, Harbin Institute of Technology, Harbin 150001, PR China

ARTICLE INFO

Article history:
Received 3 December 2012
Received in revised form 7 August 2013
Accepted 10 August 2013
Available online 24 August 2013

Keywords:
A. Polymer matrix composites (PMCs)
B. Thermomechanical properties
C. Finite element analysis (FEA)
Digital image correlation

ABSTRACT

The thermomechanical behavior of polymer matrix thermoprotective material during chemical decomposition can be recognized as the coupled temperature–diffusion–deformation problem of porous elastomers under high temperatures. A coupled solution model for the problem was developed to analyze the thermal and mechanical responses of a silica-phenolic composite exposed to heat flux environments. In the model, the coupling heat-transfer process, generation of pyrolysis gases and their subsequent diffusion process and thermal deformation were taken into account. The governing equations were established and further modified using the finite element method to obtain the effective element stiffness equation for each triangular element. The decomposition degree, displacement, thermal strain and stress distribution were calculated using the coupled solution model. Additionally, a two-dimensional digital image correlation (2D DIC) method was applied to measure the high-temperature deformation and strain of each specimen. The accuracy of the model was further assessed by comparing predicted and experimental depths of heat affected zones.

1. Introduction

Silica fiber reinforced phenolic resin matrix composites are favored in thermal protection structures of numerous vehicle and nozzles of solid rocket motor, due to their superior insulating and erosion resistant qualities [1,2]. These composites undergo thermochemical decomposition and irreversible changes of thermomechanical properties under high temperatures which adversely affect the structural integrity and reliability of the composite. Therefore, it is necessary to study the thermomechanical behavior for further research on the failure and structure design of the thermoprotective composite under high temperatures. When silica-phenolic composite is subjected to heat flux environments, the solid matrix degrades to form carbonaceous char and gaseous products which may cause internal high pore pressure. As pyrolysis reactions proceed, the porosity and permeability of the material become sufficiently large to allow the gas flow. The heat–mass transfer processes and thermal blockade phenomena are generally associated with the pyrolysis reactions of phenolic resin. In addition, the thermal expansion coefficients difference of the composite matrix and the second phase can lead to high thermal stress. In spite of their complexity and coupling, the dynamic processes have significant effect on the calculation of deformation and thermal stress field. In order to predict the thermomechanical properties of the composite, the effects of the as-mentioned processes must be considered in the formulation of an accurate model.

The sequential methods [3–7] and fully-coupled solution methods [8–12] are generally adopted to analyze the thermomechanical behavior of composite materials. The materials were exposed to the constant temperature [5], internal heat source [8,9], heat flux [3,4,10–12] and fire [6,13–16] as boundary conditions. Sullivan et al. [8–10] proposed a finite element method to study the thermochemical decomposition of polymeric materials. A similar model was introduced by Matsuura et al. [11,12]. The numerical results of temperature and strain of silica-phenolic ablator under high heating rates showed good agreements with the data of three typical experiments, named as restrained thermal growth (RTG) tests, free thermal expansion (FTE) tests and laser heating tests. A different method was presented by Mcmanus et al. [3,4] and Wu and Katsube [5]. The average compressive stress and longitudinal strain of decomposing composites were predicted by thermochemical decomposition and thermomechanical deformation analysis. However, the fully-coupled model for polymer matrix composites (PMCs) subjected to heat flux environments which actually closer to the real service environments of materials and the high-temperature deformation measurement have been rarely reported so far.

This study developed a fully-coupled model to predict the thermomechanical behavior of silica-phenolic composites during chemical decomposition. In addition, the 2D digital image correla-

* Corresponding author. Tel./fax: +86 451 86412613.
E-mail address: liangj@hit.edu.cn (J. Liang).

0266-3538/$ - see front matter © 2013 Elsevier Ltd. All rights reserved.
http://dx.doi.org/10.1016/j.compscitech.2013.08.012

tion (DIC) technique was used to measure the high-temperature deformation and strain.

2. Experimental procedure

2.1. Materials

The phenolic impregnated silica fiber composite (Aerospace Research Institute of Materials and Processing Technology, Beijing, China) was selected and characterized, in which the silica fibers were regularly woven within the fiber plane and the fiber plane was oriented perpendicular to the longitudinal axis of the cuboid specimens ($10 \times 10 \times 40$ mm). The geometrical model and boundary conditions are illustrated in Fig. 1. It is assumed that material in the fiber plane (y–z plane shown in Fig. 1) exhibits isotropic. The subscripts L and T indicate properties of solid phase in the fiber plane and in the perpendicular direction (x direction shown in Fig. 1), respectively. In this experiment, the radiant heat flux was applied perpendicular to the fiber plane and the surface convection constant was taken as 5 W/(m^2 °C).

The basic material properties, temperature-dependent thermal and transport properties of silica-phenolic composite material are summarized in Table 1. Based on the properties of virgin and char material listed in Table 1, the properties of the solid material can be calculated as a weighted function of the degree of decomposition c of the pyrolysis reaction [1,17]. The degradation of material stiffness will occur under high temperatures. Unfortunately, there is no available material stiffness degradation data of the silica-phenolic composite on hand. Therefore, the temperature-dependent stiffness property of E-glass/vinyl ester composite in Ref. [18] was also used in this paper.

2.2. Experimental

The 2D DIC method has been widely accepted and commonly used as a powerful and flexible tool for surface deformation measurement [19]. Nevertheless, the application of DIC method in high-temperature deformation measurement is limited due to the complexity of thermal environment. In this paper, the 2D DIC technique is used to measure the high-temperature deformation and strain of silica-phenolic composite subjected to one-sided heating.

Fig. 2a represents the high-temperature deformation measurement platform. The DIC testing system (VIC-3D, American Correlated Solutions Inc., US) includes CCD camera (1624×1224 pixel), white light source and computer system to process the acquired images. A cylindrical block of ultra-high temperature ceramics (UHTCs) material was heated using oxyacetylene flame and the rear temperature profile was measured using thermocouples (Ni–Cr). Furthermore, the radiant and convective heat transfer of the UHTCs block in the hot state could form the thermal environment, which, in turn, heated the silica-phenolic specimen. The mounted location of UHTCs block and graphite fixture is shown in Fig. 2b. To ensure the specimen surface was exposed to a radiant thermal environment, the distance between UHTCs block and specimen was set as 2 mm. The cold wall heat flux, q_{cw}, is determined as follows:

$$q_{cw} = \Im \Lambda T_{\text{rear}}^4 + \alpha_T (T_{\text{rear}} - T_a) \tag{1}$$

where $\Im$ is emissivity of UHTCs material and is taken as 0.8 in this paper, λ is Stefan–Boltzmann constant. T_{rear} and α_T represent the rear temperature and surface convection constant of the UHTCs block, respectively. T_a is ambient temperature. The cold wall heat flux exposing silica-phenolic specimen was calculated using measured rear temperature profile of UHTCs block and plotted in Fig. 3.

The speckle pattern of specimen surface was artificially made by spraying black and white paints before testing, as shown in Fig. 2c. An insulation slice was mounted to ensure the one-sided heating of specimen, as shown in Fig. 2d. To obtain the internal parameters of the CCD camera, a calibration process was conducted firstly. Then, the images carried the deformation information of specimen were captured each second. Finally, these images were used as input data to the computer program and further processed to obtain full-field deformations and strains of desire locations [19].

3. Formulation for the coupled temperature-diffusion-deformation problem

The thermomechanical behavior of PMCs during chemical decomposition can be recognized as the coupled temperature–diffusion–deformation (TDD) problem of porous elastomers under high temperatures. In the present study, the governing differential equations for the coupled TDD problem which involve energy conservation equation, mass conservation equation of gas phase and motion equation of solid phase were established in the plane strain state.

3.1. Energy conservation equation

The rate of decomposition of the solid material depends on temperature and activation energy, expressed by a modified Arrhenius kinetic reaction equation.

$$\frac{dc}{dt} = -A_0 c^n \exp\left(-\frac{E_a}{RT}\right) \tag{2}$$

where c is the degree of decomposition, A_0, n and E_a obtained by the thermogravimetric analysis (TGA) are the reaction rate constant, order of reaction and activation energy, respectively. The accuracy

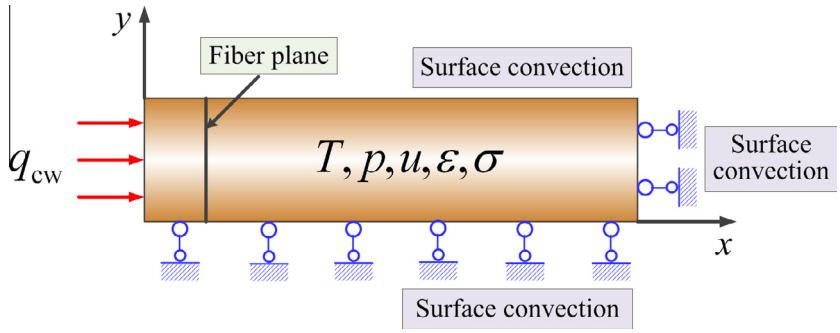

Fig. 1. The geometry model and boundary conditions.

Table 1
Material properties of silica-phenolic composites.

Properties	Value	Refs.
Density of solid material ρ_s (kg/m^3)	1270	
Reaction rate constant A_0 (kg/m^3 s)	1.94E5	TGA
Order of reaction n (–)	1.0	TGA
Activation energy E_a (J/mol)	7.88E4	TGA
Heat of decomposition Q (J/kg)	−4.187E5	TGA
Specific heat of solid material C_{ps} (J/kg K)	$1090 + 1.09\,T$	[1,2]
Specific heat of decomposition gas C_{pg} (J/kg K)	$2390 + 1.05\,T$	[1,2]
Thermal conductivity of virgin material k_{virg} (W/m K)	$0.8 + 2.76 \times 10^{-4}\,T$	[1,2]
Thermal conductivity of char material k_{char} (W/m K)	$0.96 + 8.42 \times 10^{-4}\,T - 4.07 \times 10^{-6}\,T^2$	[1,2]
Permeability of virgin material λ_{virg} (m^2)	6.18×10^{-18}	[8–10]
Permeability of char material λ_{char} (m^2)	4.85×10^{-15}	[8–10]
Gas viscosity μ (kg/ms)	$1.48 \times 10^{-5} + 2.50 \times 10^{-8}\,T$	[1,2]
Thermal expansion coefficient of virgin material β_{virg} (1/K)	4.51×10^{-5}	[1,2]
Thermal expansion coefficient of char material β_{char} (1/K)	-1.28×10^{-4}	[1,2]

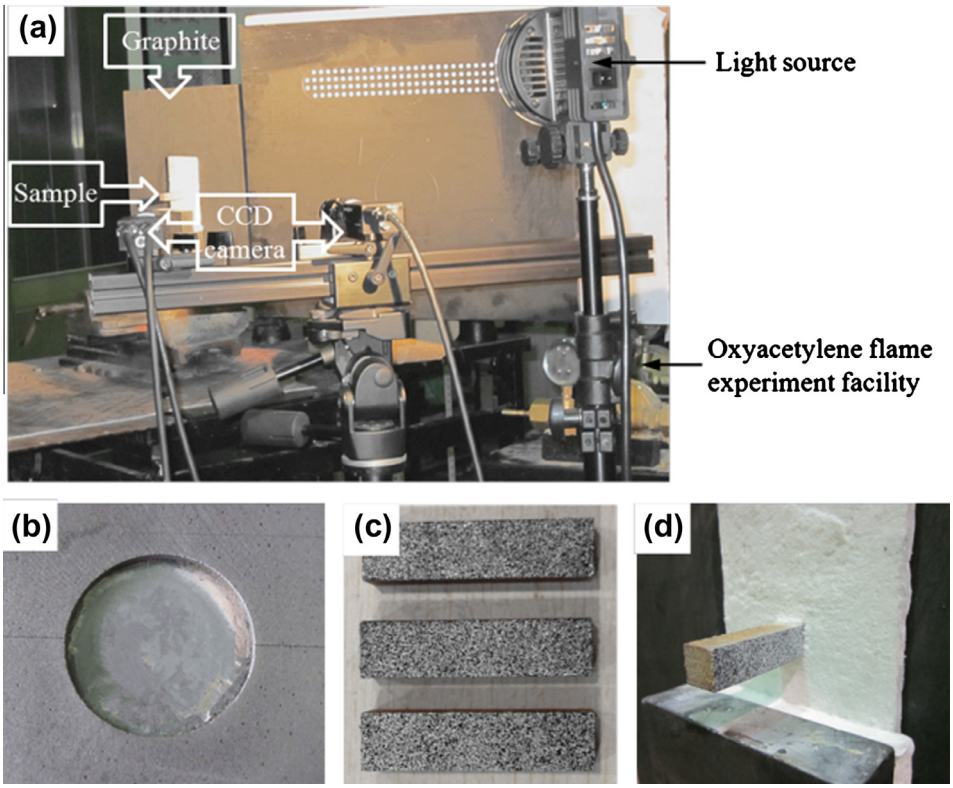

Fig. 2. High-temperature deformation measurement platform. (a) Experiment facility; (b) mounted location of UHTCs block and graphite fixture; (c) speckle pattern of specimen surface; (d) insulation slice.

of the kinetic rate Eq. (2) has been evaluated by comparing the calculated and experimental mass loss curves in Ref. [17].

For the two-dimensional heat and mass transfer problem, the energy conservation is given by a modified Laplace's equation.

$$\rho_s C_{ps}\frac{\partial T}{\partial t} = \left(k_T\frac{\partial^2 T}{\partial x^2} + k_L\frac{\partial^2 T}{\partial y^2}\right) - \rho_s C_{pg}\left[\left(-\frac{\lambda_T}{\mu_T}\frac{\partial p}{\partial x}\right)\frac{\partial T}{\partial x} + \left(-\frac{\lambda_L}{\mu_L}\frac{\partial p}{\partial y}\right)\frac{\partial T}{\partial y}\right] - Q\rho_s\frac{dc}{dt} \quad (3)$$

where k, C_p and Q are the thermal conductivity, specific heat and the heat of decomposition, respectively. The subscripts s and g represent the solid phase and gas phase, respectively. The first term on the left side of Eq. (3) represents the heat flux applied on the material surface. The second term gives the change of the internal energy of materials. Moreover, the three terms on the right side of Eq. (3) are associated with the heat conduction, convective heat transport and resin decomposition, respectively. The second term on the right side is determined through Darcy's law and expressed in terms of pressure p, permeability of material λ and gas viscosity in pores μ.

3.2. Mass conservation equation of gas phase

A representative volume element (RVE) is chosen to analyze the mass-transfer process of pyrolysis gases during decomposition. According to the mass conservation principle of gas phase, the differential equation governing the diffusion of pyrolysis gases through a porous solid material is given as:

$$\frac{\partial m_g}{\partial t} = \frac{\partial m_{pg}}{\partial t} - \rho_g\left[\frac{\partial}{\partial x}\left(-\frac{\lambda_T}{\mu_T}\frac{\partial p}{\partial x}\right) + \frac{\partial}{\partial y}\left(-\frac{\lambda_L}{\mu_L}\frac{\partial p}{\partial y}\right)\right] \quad (4)$$

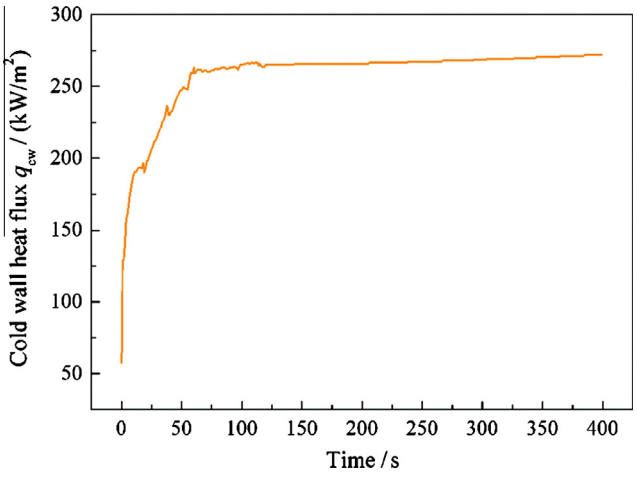

Fig. 3. The cold wall heat flux versus time.

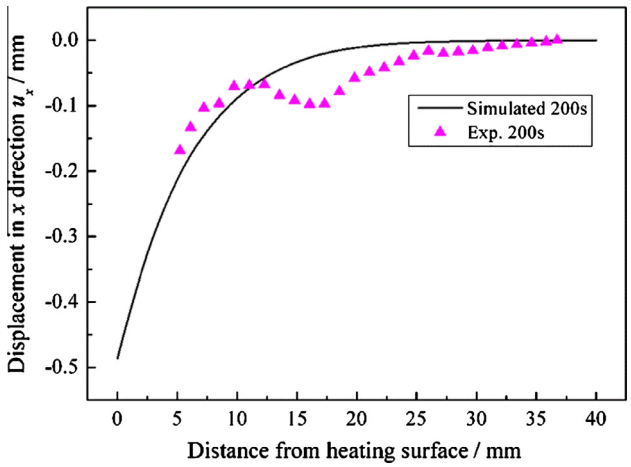

Fig. 5. Variation of experimental and simulated displacement in x direction versus d.

where m_{pg} is the gas mass generated in pyrolysis reactions. The left side of Eq. (4) is the time rate of gas storage in the solid materials. The first term on the right side gives the time rate of gas generation, which can be calculated by Eq. (2). The second term is the rate of change of the gas mass flux through the RVE.

3.3. Motion equation of solid phase

Based on the elasticity theory, the motion equation of the porous elastomers in the absence of body forces and under quasi-static conditions is expressed as follows:

$$\sigma_{ij,j} = 0 \tag{5}$$

where σ_{ij} is the total stress tensor. As in Wu and Sullivan [5,8], the effective stress law for overall strain proposed by Carroll [20] is used and the total stress is obtained.

$$\sigma_{ij} = C_{ijkl} e_{kl} - \alpha \delta_{ij} p \tag{6}$$

where α is the poroelasticity parameter and taken as 1.0 in this paper. The total thermal strains ε_{ij} are related to the elastic strains e_{ij}, expressed as follows:

$$\begin{aligned} &e_{xx} = \varepsilon_{xx} - \beta_T \Delta T, \quad e_{yy} = \varepsilon_{yy} - \beta_L \Delta T, \quad e_{zz} = -\beta_L \Delta T \\ &e_{xy} = \varepsilon_{xy}, \quad e_{yz} = \varepsilon_{yz}, \quad e_{xz} = \varepsilon_{xz} \end{aligned} \tag{7}$$

where β is the thermal expansion coefficient of the solid material.

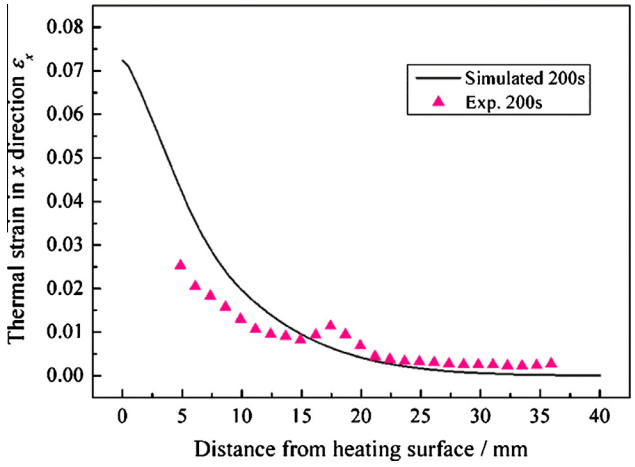

Fig. 6. Variation of experimental and simulated in-plane thermal strain versus d.

For transversely isotropic materials where the plane of isotropy is the y–z plane, there are five independent elastic constants C_{11}, C_{12}, C_{22}, C_{23} and C_{55}, where y–z plane exhibits isotropic. The motion equation of solid phase can be rewritten in x and y direction, respectively. In x direction, Eq. (5) reduces to:

$$\sigma_{xx,x} + \sigma_{xy,y} = 0 \tag{8}$$

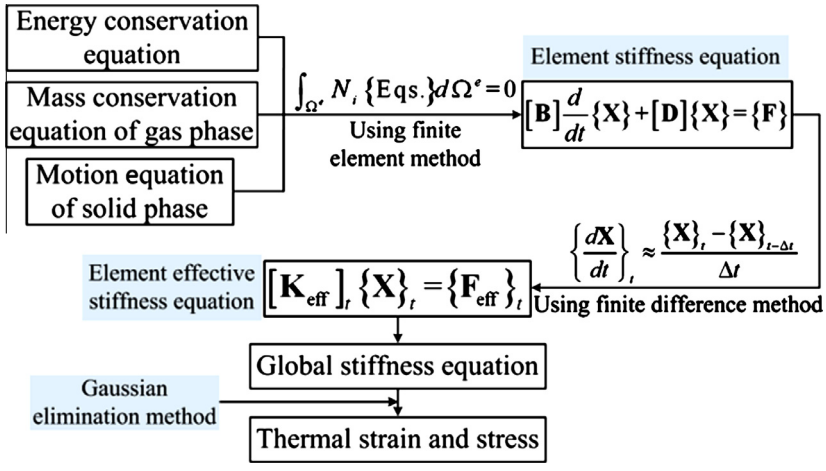

Fig. 4. Solving strategy for the coupled TDD problem.

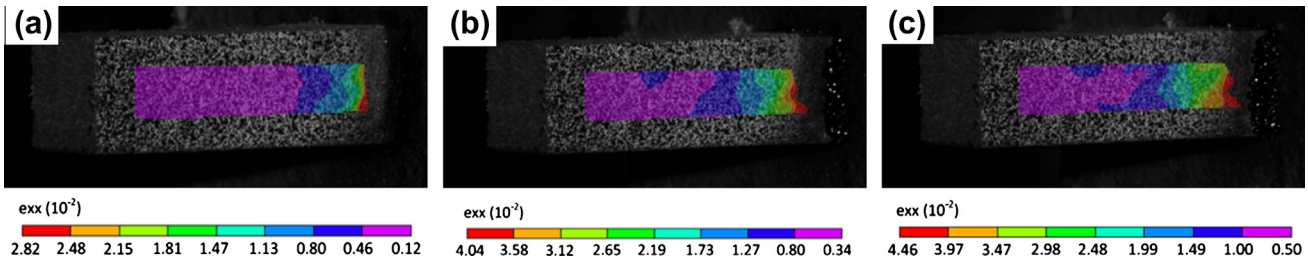

Fig. 7. Thermal strain contours of silica-phenolic specimens obtained by the DIC method at different heating time. (a) 100 s; (b) 200 s; (c) 400 s.

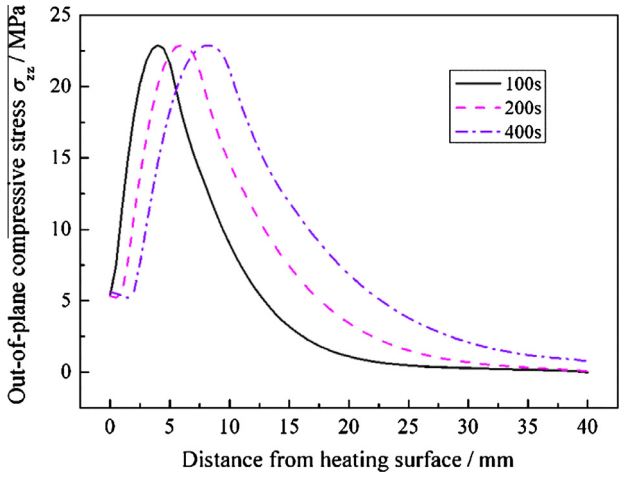

Fig. 8. Variation of simulated out-of-plane compressive stress versus *d*.

Combining Eqs. (6) and (7) and the strain–displacement relations, Eq. (8) becomes:

$$C_{11}u_{x,xx} + C_{12}u_{y,yx} + C_{55}(u_{x,yy} + u_{y,xy}) - (C_{11}\beta_T + 2C_{12}\beta_L)T_{,x} - \alpha p_{,x} = 0 \quad (9)$$

Similarly, the motion equation in y direction can be written as:

$$C_{22}u_{y,yy} + C_{12}u_{x,xy} + C_{55}(u_{y,xx} + u_{x,yx}) - (C_{22}\beta_L + C_{12}\beta_T + C_{23}\beta_L)T_{,y} - \alpha p_{,y} = 0 \quad (10)$$

3.4. Boundary conditions

The initial pressure and temperature of the specimen are 0.1 MPa and 20 °C, respectively. Prescribed heat flux and mechanical boundary conditions as expressed in Eqs. (11) and (12), respectively, were considered in the present model.

$$-k\frac{\partial T(x,t)}{\partial x}\Big|_{x=0} = q_w \quad (11)$$

$$u(x,y)|_{x=L} = 0, \quad v(x,y)|_{y=0} = 0 \quad (12)$$

where q_w is the radiant heat flux perpendicular to the specimen surface.

4. Calculation process using finite element method

Since the four variables of temperature T, pore pressure p and displacements u_x, u_y are coupled in the above-mentioned governing differential equations, solution of these equations is accomplished using the finite element method. Eqs. (3), (4), (9), and (10) are rewritten as the integral forms [8–10].

$$\int_{\Omega^e} N_i\{\text{Eqs. } (3),(4),(9),(10)\}d\Omega^e = 0 \quad (13)$$

where N_i is the shape function of element and Ω^e is the element volume. The constant-strain triangular elements are adopted. The node and element number are artificially made to reduce the bandwidth of global stiffness matrix. Thus, the coupled matrix form can be obtained by rearranging Eq. (13).

$$[\mathbf{B}]_{4\times4}\frac{d}{dt}\{\mathbf{X}\}_{4\times1} + [\mathbf{D}]_{4\times4}\{\mathbf{X}\}_{4\times1} = \{\mathbf{F}\}_{4\times1} \quad (14)$$

where $\{\mathbf{X}\}$ is the desired solving variables.

$$\{\mathbf{X}\} = \{T, p, u_x, u_y\}^T \quad (15)$$

After the time derivative terms of Eq. (14) are eliminated using the finite difference method, the effective element stiffness equation for each triangular element can be established.

$$[\mathbf{K}_{\text{eff}}]_{4\times4}\{\mathbf{X}\}_{4\times1} = [\mathbf{F}_{\text{eff}}]_{4\times1} \quad (16)$$

where $[\mathbf{K}_{\text{eff}}]$ and $[\mathbf{F}_{\text{eff}}]$ are the effective stiffness matrix and effective force vector, respectively. Subsequently, the global stiffness equation is assembled and solved by Gaussian elimination method. Thus, the temperature, pore pressure and displacement for each triangular element can be determined. The thermal strain and stress of the element are further obtained using displacement–strain relations and constitutive equations. The solving strategy for the coupled problem is explicitly given in Fig. 4.

5. Results and discussion

The mathematical model developed in Section 4 was used to calculate the thermomechanical response of silica-phenolic composite applied the experimental heat flux condition as shown in Fig. 3. The curve of displacement in x direction versus distance from heating surface (named as d) at the heating time of 200 s is plotted in Fig. 5 along with the measured results obtained by the DIC method. It should be pointed out that the displacement vector

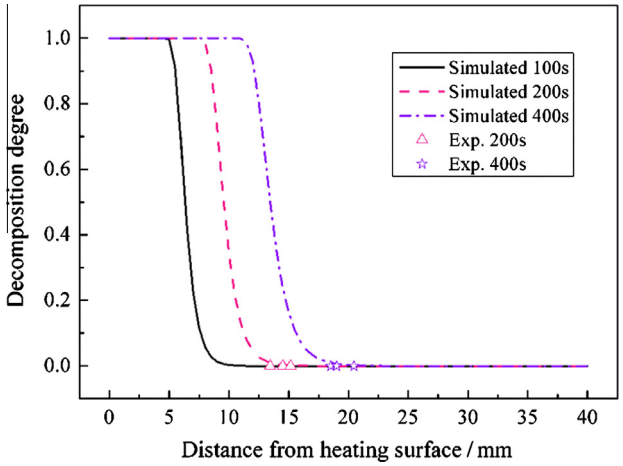

Fig. 9. Dependence of simulated decomposition degree on *d* and measured depths of heat affected zones.

u_x is negative in the current coordinates. The absolute maximum in-plane displacement is 0.49 mm. Comparing the experimental and simulated value, the measured displacements at the location where d 12.5–22.5 mm deviate from the calculated values slightly, while the measured displacement are in good agreement with the simulated results at other locations.

Fig. 6 shows the variation of experimental and simulated thermal strain ε_{xx} versus d at 200 s. There is a quite good agreement between the predicted and experimental values except of the thermal strain at location where d 15–20 mm. With the increasing of d, the thermal strain decreases correspondingly and exhibits an exponent tendency in x direction of materials. In addition, it should be noted that Figs. 5 and 6 demonstrate non-monotonicity of displacement and thermal strain of the material. The material response can be divided into three temperature regions: the thermoelastic, transition and poroelastic regions [8–10]. The material temperatures at location of 15–20 mm from the heated surface are in the transition region. Owing to breaking down of the cross linking between the molecular chains and the material softening, the displacement and thermal strain of the material increase slightly. Furthermore, in the transition region decomposition gases begin to accumulate and the initial effect of the pore pressure on the material response becomes apparent [8–10]. The thermal strain contours of silica-phenolic specimens obtained by the 2D DIC method are presented in Fig. 7. A gradient change in thermal strain with d is clearly shown in the figure.

Fig. 8 illustrates the calculated out-of-plane compressive stress distribution of materials at 100, 200 and 400 s, respectively. The maximum thermal stress is 22.8 MPa at 100 s and the changes in maximum stresses with the increasing of the heating time are small. Since the thermal expansion can lead to high thermal stress during the pyrolysis reactions of phenolic resin, the location of the maximum stress does not appear at the intensive ablative surface.

Fig. 9 shows the variation of the calculated decomposition degree versus d and measured depths of heat affected zones of specimens. The values of the decomposition degree, 1 and 0, indicate that the pyrolysis reactions have completed and not happened, respectively. The figure also gives the comparison of the depths of heat affected zones for predicted results with the measured values of the specimens sliced after testing. The measured depth of heat affected zone of a specimen is 20.45 mm at 400 s, while that of calculated value is 19.5 mm. Moreover, the heat affected zone penetrates further into the virgin material with the increasing of the heating time, attributed to heat-transfer process in the material.

It is noted that the storage of decomposition gases tends to reduce the temperatures, which, in turn, retards the decomposition reactions and the rate of gas generation [1,2,17]. And the porosity of the decomposing, expanding polymer composite which affects gas storage is dependent on the content of filler. Therefore, the importance of influence of filler on the pyrolysis process cannot be neglected. Additionally, the discrepancies which do exist between the calculated and experimental results mentioned above are thought to be due to the fact that the model does not account for all of the physical processes which occur in the material. For example, it is assumed that the decomposition gases are non-reactive in the model. In certain cases, this assumption may have significant effect on the results. The mathematical model could be further improved by including some of important physical processes in our future work.

6. Conclusions

The mathematical formulas for the coupled TDD problem in the plane strain state were established. A coupled solution method for the problem was developed to predict the thermal and mechanical responses of silica-phenolic composite subjected to heat flux environments. The high-temperature deformation measurements were conducted to assess the accuracy of the multiphysics field coupling model. Comparing the numerical and experimental results of displacements and thermal strains, the proposed model can satisfactorily predict the thermomechanical behavior of the PMCs. With the increasing of d, the displacement and thermal strain decrease. The thermal stress has a local peak during chemical decomposition and the peak moves towards the back surface of the material with the increasing of the heating time.

The decomposition of resin matrix may lead to crack propagation and delamination which adversely affect the structural integrity of the composite. It is, of course, possible to utilize the coupled model, in conjunction with material strength degradation data, to predict the failure of PMCs due to internal thermal stress.

Acknowledgment

This work is supported by the National Natural Science Foundation of China under Grant Nos. 90916027 and 11102051.

References

[1] Henderson JB, Tant MR, Doherty MP, et al. Characterization of the high-temperature behaviour of a glass-filled polymer composite. Composites 1987;18:205–15.
[2] Henderson JB, Wiecek TE. A mathematical model to predict the thermal response of decomposing, expanding polymer composites. J Compos Mater 1987;21:373–93.
[3] McManus LN, Springer GS. High temperature thermomechanical behavior of carbon–phenolic and carbon–carbon composites, I. Analysis. J Compos Mater 1992;26:206–29.
[4] McManus LN, Springer GS. High temperature thermomechanical behavior of carbon–phenolic and carbon–carbon composites, II. Results. J Compos Mater 1992;26:230–51.
[5] Wu Y, Katsube N. A constitutive model for thermomechanical response of decomposing composites under high heating rates. Mech Mater 1996;22:189–201.
[6] Bai Y, Keller T. Modeling of mechanical response of FRP composites in fire. Composites A 2009;40:731–8.
[7] Kandare E, Kandola BK, Myler P, Edwards G. Thermo-mechanical responses of fiber-reinforced epoxy composites exposed to high temperature environments. Part I: experimental data acquisition. J Compos Mater 2010;44:3093–114.
[8] Sullivan RM, Salamon NJ. A finite element method for the thermochemical decomposition of polymeric materials – I. Theory. Int J Eng Sci 1992;30:431–41.
[9] Sullivan RM, Salamon NJ. A finite element method for the thermochemical decomposition of polymeric materials – II. Carbon phenolic composites. Int J Eng Sci 1992;30:939–51.
[10] Sullivan RM. A coupled solution method for predicting the thermostructural response of decomposing, expanding polymeric composites. J Compos Mater 1993;27:408–34.
[11] Matsuura Y, Hirai K. A challenge of predicting thermo-mechanical behavior of ablating SiFRP with finite element analysis. In: 46th AIAA/ASME/SAE/ASEE joint propulsion conference and exhibit, Nashville, Tennessee; 2010.
[12] Matsuura Y, Hirai K, Kamita T, et al. A challenge of modeling thermo-mechanical response of silica-phenolic composites under high heating rates. In: 49th AIAA aerospace sciences meeting, Orland, Florida; 2011.
[13] Asaro RJ, Lattimer B, Ramroth W. Structural response of FRP composites during fire. Compos Struct 2009;87:382–93.
[14] Gibson AG, Torres MEO, Browne TNA, et al. High temperature and fire behaviour of continuous glass fibre/polypropylene laminates. Composites A 2010;41:1219–31.
[15] Feih S, Mouritz AP, Mathys Z, Gibson AG. Tensile strength modeling of glass fiber–polymer composites in fire. J Compos Mater 2007;41:2387–410.
[16] Shokrieh MM, Abdolvand H. Three-dimensional modeling and experimental validation of heat transfer in polymer matrix composites exposed to fire. J Compos Mater 2011;45:1953–65.
[17] Shi SB, Liang J, Yi FJ, Fang GD. Modeling of one-dimensional thermal response of silica-phenolic composites with volume ablation. J Compos Mater 2012. http://dx.doi.org/10.1177/0021998312454907.
[18] Kim J, Lee SW, Kwon S. Time-to-failure of compressively loaded composite structures exposed to fire. J Compos Mater 2007;41:2715–35.
[19] Pan B, Qian K, Xie H, et al. Two-dimensional digital image correlation for in-plane displacement and strain measurement: a review. Meas Sci Technol 2009;20:1–17.
[20] Carroll MM. An effective stress law for anisotropic elastic deformations. J Geophys Res 1979;84:7510–2.